Journal of Colloid and Interface Science 464 (2016) 153–159

Contents lists available at ScienceDirect

Journal of Colloid and Interface Science

journal homepage: www.elsevier.com/locate/jcis

Short Communication

Enhanced interlayer trapping of a tetracycline antibiotic within montmorillonite layers in the presence of Ca and Mg

Ludmilla Aristilde [a,*], Bruno Lanson [b], Jocelyne Miéhé-Brendlé [c], Claire Marichal [c], Laurent Charlet [b]

[a] Department of Biological and Environmental Engineering, College of Agricultural and Life Sciences, Cornell University, Ithaca, NY 14853, USA
[b] Institut des Sciences de la Terre, ISTerre, Univ. Grenoble-Alpes, CNRS, F-38041 Grenoble, France
[c] Equipe Matériaux à Porosité Contrôlée, IS2M, CNRS 7361, Université de Haute Alsace, 68093 Mulhouse, France

GRAPHICAL ABSTRACT

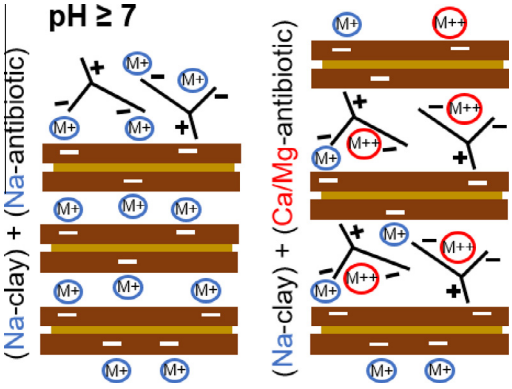

ARTICLE INFO

Article history:
Received 17 October 2015
Revised 11 November 2015
Accepted 12 November 2015
Available online 14 November 2015

Keywords:
Antibiotics
Montmorillonite
Interlayer adsorption
Aqueous conditions
Cation-promoted adsorption

ABSTRACT

The formation of a ternary antibiotic–metal–clay complex is hypothesized as the primary adsorption mechanism responsible for the increased adsorption of tetracycline antibiotics on smectites in the presence of divalent metal cations under circumneutral and higher pH conditions. To evaluate this hypothesis, we conducted a spectroscopic investigation of oxytetracycline (OTC) interacting with Na-montmorillonite in the presence and absence of Ca or Mg salts at pH 6 and pH 8. Despite a two-fold increase in OTC adsorbed in the presence of Ca or Mg, both solid-state nuclear magnetic resonance and infrared signatures of the OTC functional groups involved in metal complexation implied that the formation of an inner-sphere ternary complexation was not significant in stabilizing the adsorbate structures. The spectroscopic data further indicated that the positively-charged amino group mediated the OTC adsorption both in the absence and presence of the divalent metal cations. Focusing on the experiments with Mg, X-ray diffraction analysis revealed that the metal-promoted adsorption was coupled with an increased intercalation of OTC within the montmorillonite layers. The resulting interstratified clay layers were characterized by simulating X-ray diffraction of theoretical stacking compositions using molecular dynamics-optimized montmorillonite layers with and without OTC. The simulations uncovered the evolution of segregated interstratification patterns that demonstrated how increased access to smectite interlayers in the presence of the divalent metal cations enhanced adsorption of OTC. Our findings suggest that specific aqueous structures of the clay crystallites in response to the co-presence of Mg and OTC in solution served as precursors to the interlayer trapping of the antibiotic species. Elucidation of these structures is needed for further insights on how aqueous chemistry

* Corresponding author.
E-mail address: ludmilla@cornell.edu (L. Aristilde).

http://dx.doi.org/10.1016/j.jcis.2015.11.027

influences the role of smectite clay minerals in trapping organic molecules in natural and engineered soil particles.

1. Introduction

Due to the widespread use of tetracycline (TC) antibiotics in both human and veterinary medicine as well as in livestock maintenance, these antibiotics have been detected in environmental matrices worldwide [1–4]. A major entry route of TC antibiotics into the environment is via the application of antibiotic-containing manure or wastewater sludge on agricultural soils [5–7]. In addition to the transfer of antibiotic-resistance genes from contaminated wastes to soils [8–10], there are concerns over the accumulation of TC antibiotics in soils and sediments [11–14] due to their potential disruption of microbial processes [15–21] and uptake by vegetable crops [22,23]. Therefore, it is important to elucidate the mechanisms that govern the retention of TC antibiotics within soil particles, a knowledge that can also benefit the engineering of effective antibiotic adsorbents.

Adsorption of TC antibiotics on different soils demonstrated highest retention of the antibiotics in soils enriched in clay minerals [11], especially when the soil organic content is relatively low [24]. Compared to non-swelling clays, smectite-type clays exhibited higher sorption capacity for TC antibiotics due to their high cation-exchange capacity and swelling capabilities [25–28]. Solvation of charge-compensating cations induces an increase in the layer-to-layer distance (d_{001}) in smectite interlayers, which subsequently accommodate interlayer adsorption of the organic species [29]. The adsorption of TC antibiotics to Na-saturated smectites including montmorillonite (MONT) was shown to be pH-dependent, with highest adsorption occurring at acidic pH when the antibiotic species are cationic (Fig. 1A) [27,30–34]. Infrared (IR) and solid state nuclear magnetic resonance (NMR) analyses confirmed a cation-exchange adsorption mechanism involving the protonated dimethyl amino group in TC antibiotics (Fig. 1A) [31,32]. Moreover, X-ray diffraction (XRD) data demonstrated that the pH-dependent adsorption correlated positively with intercalation of the antibiotic species within the Na-smectite interlayers [30–32,34–36]. Thus, at circumneutral and basic pH conditions, interlayer adsorption of TC antibiotics was found to be minimal [31,34].

However, in the presence of divalent metal cations that are ubiquitous in the soil matrix, TC adsorption on smectite clays can be enhanced [25,30,32,37,38]. The prevailing hypothesized mechanism is that the formation of a strong ternary antibiotic–metal–clay complex facilitates stable interactions between negatively-charged antibiotic species and the negatively-charged clay surface [25,38]. In support of this hypothesis, TC adsorption was found to be greater on Ca-MONT than on Na-MONT under pH conditions where the second ionizable group known to be involved in metal complexation is deprotonated (pH ⩾ 7) [38]. However, the occurrence of the hypothesized metal–bridging interaction has not yet been confirmed. Therefore, molecular spectroscopic investigations are still warranted to fully examine the underlying adsorption mechanisms in the presence of divalent metal cations.

A second possible mechanism is that the divalent metal cations facilitate interlayer adsorption of the antibiotic species [38]. Under low hydration conditions, Ca-smectites are expected to have a higher d_{001} than Na-smectites due to the greater amount of water molecules in the solvation shell of Ca than in the Na solvation shell [39]. The recorded XRD patterns of Ca–Na smectites revealed demixing (or interstratification) of Ca-interlayers with Na-interlayers, as a

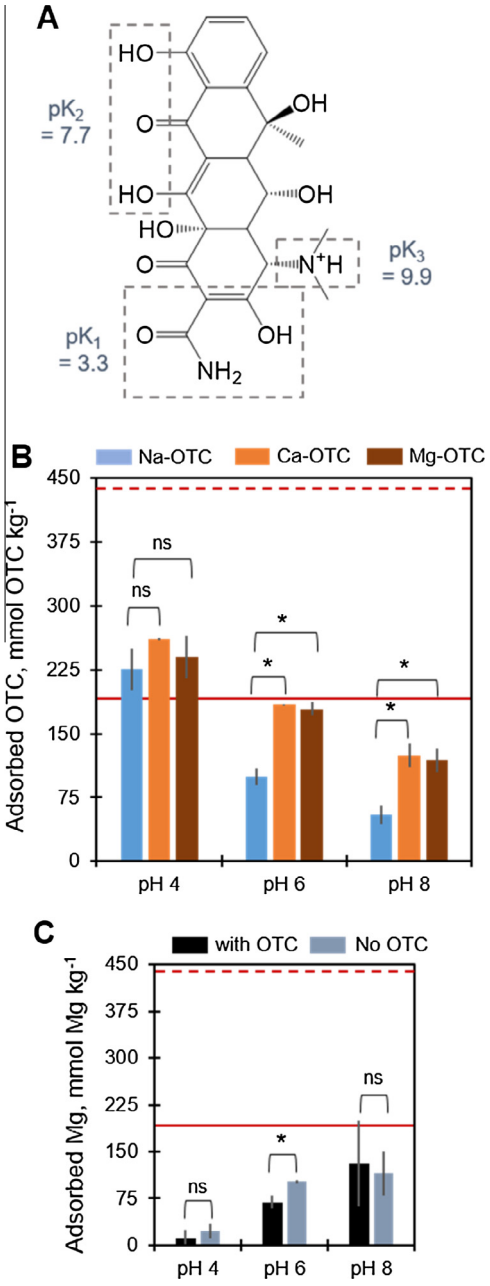

Fig. 1. (A) Chemical structure of OTC showing the ionizable groups and their reported pK_a values. (B) Amount of adsorbed OTC on MONT (mmol OTC kg^{-1}) in the absence (blue) and the presence of Ca (orange) or Mg (brown) at pH 4, pH 6, and pH 8. (C) Amount of adsorbed Mg OTC adsorbed on MONT (mmol Mg C kg^{-1}) in the presence (brown) and absence (blue) of OTC. In A and B, the horizontal red lines represent the value for the permanent charge (dashed line, 440 mmol$_c$ kg^{-1} clay) and the variable charge on the clay (solid line, 190 mmol$_c$ kg^{-1} clay); clay variable charge is prominent at pH ⩾ 7. The same concentration of OTC (320 μM) was used in all the experiments. For the experiments with the metals (Ca or Mg), equimolar concentrations of OTC and metals were used. Data (average ± standard deviation) are from 3 to 5 independent replicates. Statistical analysis using unpaired *t*-test: * $p < 0.03$; ns, not statistically significant.

result of the different hydration states of the cations in smectite interlayers [40–44]. The interstratification pattern could be characterized as random or segregated based on the evolution of the 001 peak [45]. Previous XRD data presented segregated-type interstratification patterns for both Ca-MONT and Na-MONT intercalated with oxytetracycline (OTC), a veterinary TC antibiotic [38]. The underlying antibiotic intercalation behavior within the OTC-exchanged MONT layers in the presence of Ca and other divalent cations has not been fully characterized.

With respect to the pH-dependent intercalation of OTC within Na-MONT layers, a previous study [34] has employed a combination of experimental and simulated XRD to characterize the interstratification of Na- and OTC-MONT layers. The intercalation of OTC within the Na-MONT interlayers was found to be random at pH 4 and pH 5 but segregated at pH 6 and pH 8 [34]. This segregation pattern could not be explained solely by the relative distribution of cationic versus anionic OTC species [34]. Instead, in addition to the speciation of the antibiotic species, it was proposed that pH-dependent formation of MONT crystallites with unexfoliated layers was responsible for the decrease in OTC interlayer adsorption as pH increases [34]. Therefore, it is possible that the divalent metal cations may induce increase in OTC interlayer adsorption by altering MONT aggregation chemistry, irrespective of the formation of a ternary complex. This third possible mechanism has received little attention.

In this short communication, we seek to shed light on the role of the three aforementioned mechanisms in increasing OTC adsorption onto Na-MONT in the presence of Ca or Mg at pH 6 and pH 8. We characterized the resulting OTC-MONT adsorbate structures using a combination of IR, NMR, and both experimental and simulated XRD. As a pre-requisite to the cation-promoted adsorption of OTC, our spectroscopic results did not support the occurrence of a strong ternary complexation, but our XRD analysis revealed that an enhanced access of OTC to the MONT interlayers was essential. Moreover, the spectroscopic analysis indicated that the intercalated OTC in the presence of the divalent cations was adsorbed via similar adsorption mechanisms occurring in the absence of the divalent cations. Follow-up XRD simulations presented the theoretical composition of OTC-exchanged MONT layers responsible for the evolution of segregated interstratification as a function of increasing Mg. The present findings stress the need to elucidate further the structural responses of clay crystallites to different aqueous chemistry as a precursor to interlayer trapping of antibiotics and other ionizable contaminants in smectite-type clay minerals.

2. Experimental section

The experimental methods are described briefly below. Detailed descriptions are presented in previous publications [31,34].

2.1. Adsorption experiments

In 50-mL PTFE tubes, 20 mL of 320 μM OTC was reacted with 20 mg Na-MONT. This clay mineral was previously determined [46] to have a total cation-exchange capacity of 630 $mmol_c\ kg^{-1}$ clay: a permanent structural charge of 440 $mmol_c\ kg^{-1}$ clay and a variable charge of 190 $mmol_c\ kg^{-1}$ clay. The OTC solutions were prepared with a background solution containing 0.01 M $NaNO_3$ with 5 mM each of an acetate/bicarbonate ($NaCH_3COO/NaHCO_3$) buffer, adjusted to pH 4.0, 6.0, or 8.0 by HNO_3 additions. The solution pH was maintained within 0.1 pH unit of the starting pH over the 40-h course of the adsorption experiments. Following centrifugation and filtering of the OTC-clay suspensions, the OTC concentration in the supernatants was determined by UV–vis analysis (356 nm at pH 4 and pH 6; 360 nm at pH 8) using a Perkin-Elmer Lambda35 spectrophotometer. For reactions of Na-MONT with metal-complexed OTC at the different pH values, the OTC solutions were prepared as described above with equimolar concentrations of OTC and either $Ca(NO_3)_2$ or $Mg(NO_3)_2$. The amount of Ca or Mg adsorbed was determined by inductively coupled plasma optical emission spectroscopy (ICP-OES) Perkin Elmer OPTIMA 3300 DV; detection limit = 10 ppb).

2.2. Solid-state FTIR and NMR measurements

The OTC-MONT samples obtained at pH 8, both in the absence and presence of the divalent cations, were examined by FTIR and NMR spectroscopies as detailed previously [31]. The FTIR measurements were conducted using a Bruker Equinox 55 spectrometer with a DTGS detector. The $^{1}H–^{13}C$ cross-polarization magic angle spinning (CPMAS) NMR spectra were recorded with a Bruker Avance II 400WB instrument. Spectrometer settings and sample handling were as described previously [31].

2.3. Experimental and simulated XRD

Oriented samples of the OTC-clay suspensions were equilibrated and measured at constant temperature (25 °C) and relative humidity (20%). This RH value was previously shown to be optimal for monitoring changes in d_{001} during interstratification of Na- and OTC-exchanged MONT layers [34]. The XRD patterns were recorded with a Bruker D5000 diffractometer (0.02° 2θ step size and 8 s as counting time per step) operated at 40 kV and 40 mA and equipped with a SolX solid-state detector (Baltic Scientific Instruments) and an Ansyco rh-plus 2250 humidity control device with an Anton Paar TTK450 chamber.

To characterize the OTC-MONT interstratified layers in the presence and absence of Mg, we obtained simulated XRD profiles of theoretical layer compositions with different proportions of Na-MONT and OTC-MONT [34]. Details of this procedure are previously described by Aristilde et al. [34]. Briefly, the *z*-coordinates of molecular dynamics-optimized adsorptive species in Na-MONT and OTC-MONT were used to simulate XRD profiles assuming either random or segregated interstratification pattern [34].

3. Results and discussion

3.1. Effects of divalent cations on OTC adsorption

In agreement with previous studies [27,30–34], the OTC adsorption on Na-MONT was the highest at pH 4 and the lowest at pH 8 (Fig. 1B). In the presence of Ca or Mg, the adsorption of OTC on Na-MONT was increased at both pH 6 and pH 8 (Fig. 1B). Compared to the adsorption of OTC in the absence of divalent cations, the divalent cation-promoted adsorption was up to 80% more at pH 6 and 120% more at pH 8 (Fig. 1B). These findings are consistent with previous reports that the adsorption of TC antibiotics on Ca-MONT was greater than the adsorption on Na-MONT [38]. However, when MONT was saturated with Ca in these previous studies, the divalent cation inhibited the antibiotic adsorption at acidic pH, presumably by competing with the cation-exchange adsorption mechanism. By contrast, our data at pH 4 revealed similar adsorption for OTC in the absence and presence of Ca or Mg (Fig. 1B). Therefore, we present an aqueous condition with a 1:1 divalent cation: antibiotic ratio in solution that can promote TC adsorption on Na-MONT at unfavorable high pH without compromising adsorption at favorable low pH (Fig. 1B).

We also obtained the amount of Mg under the same pH conditions discussed above, both in the presence and absence of OTC

(Fig. 1C). At pH 4, there was minimal adsorbed Mg (up to 27 mmol Mg kg^{-1} clay) compared to adsorbed OTC (up to 261 mmol OTC kg^{-1} clay) (Fig. 1C). This further indicated that Mg in the 1:1 Mg:OTC solution did not interfere with OTC adsorption at pH 4. In the presence of OTC at pH 6 and pH 8, the amount of adsorbed Mg was increased considerably with, on average, 60 and 131 mmol Mg kg^{-1} clay respectively at pH 6 and pH 8 (Fig. 1C). The amount of adsorbed Mg was also increased significantly in the absence of OTC with increasing pH (Fig. 1C). Therefore, the co-sorption of Mg with OTC at pH 6 and pH 8 could be due to increasing negatively-charged sites on the clay edges, in addition to the possible formation of a strong ternary complex between the clay surface and the metal-complexed OTC.

3.2. Spectroscopic analysis via FTIR and NMR

To probe the underlying OTC adsorption mechanisms in the presence of divalent cations, we analyzed the adsorbate structures at pH 8 in the absence and presence of Ca or Mg using FTIR and $^{1}H–^{13}C$ CPMAS NMR (Fig. 2). Generally, we observed slightly weaker intensities in both FTIR and NMR spectra for MONT-Mg-OTC than for MONT-Ca-OTC (Fig. 2). A previous study [32] reported a systematic decrease in peak intensity in FTIR spectra of OTC-MONT as a function of increasing adsorbed OTC on Na-MONT in the absence of divalent cations. Therefore, the difference in peak intensities in our data may be due, relative to the MONT-Ca-OTC sample, to the MONT-Mg-OTC sample having slightly less adsorbed OTC leading to reduced resolution of the vibration bands and nuclei resonances in OTC. On average, as illustrated in Fig. 1B, we did obtain a slightly higher amount of adsorbed Ca-OTC than Mg-OTC at both pH 4 and pH 8 but this difference was not statistically significant, when taking into account all the independent replicate measurements.

With respect to the localization of observable IR bands in OTC in the absence and presence of the divalent metal cations, there were no differences in the IR bands of the functional groups known to be associated with metal complexation: the C═O amide I stretching band at 1669 cm^{-1} (a), the C═C stretching band at 1583 cm^{-1} (b), and the phenolic C—O stretching band at 1178 cm^{-1} (g) (Fig. 2A and B). This implied that a strong inner-sphere ternary complexation between metal-complexed OTC and the clay surface was not likely in both MONT-Ca-OTC and MONT-Mg-OTC. Because outer-sphere complexation through water bridges may not alter the IR bands, our FTIR data could not rule out the formation of this weaker ternary complexation. Our FTIR data further revealed that the dimethylamino group in OTC mediated the adsorption mechanism both in the absence and presence of the divalent cations (Fig. 2A and B). As was shown previously [31], the participation of this amino group in adsorption was confirmed by the disappearance of the CH_3 vibration band at 1456 cm^{-1} (d) and the appearance of a doublet CH_3 vibration bands at 1506 and 1475 cm^{-1} (Fig. 2A and B) [31]. Accordingly, compared to the $^{1}H–^{13}C$ CPMAS NMR of the OTC alone, the broadening of the C_{32} and C_{33} resonances indicated lower mobility of these CH_3 moieties in OTC-MONT at pH 8 both in the absence and presence of Ca or Mg (Fig. 2A and C).

The modifications in the resonances corresponding to C_3, C_9, and C_{11} in MONT-OTC at pH 8 were previously attributed to the deprotonation of the OH functional group attached to C_9 [31]. Subsequent changes in these resonances would result from the formation of a strong ternary cation-mediated complexation between the OTC (via the deprotonated functional group of $pK_a = 7.7$) and the clay. Previous liquid-state ^{1}H NMR studies on the interaction of Ca or Mg with OTC attributed broadening of the peaks to OTC aggregation [47]. When compared to the $^{1}H–^{13}C$ CPMAS NMR spectrum of MONT-OTC, the corresponding spectrum of MONT-Mg-OTC showed no appreciable differences in the signal peaks for C_3, C_9, and C_{11} (Fig. 2A and C). However, the broadness of these signals in the MONT-Mg-OTC indicated a reduced mobility of OTC, which is consistent, as previously suggested, with OTC aggregation at the mineral surface [47]. With respect to the MONT-Ca-OTC $^{1}H–^{13}C$ CPMAS NMR spectrum, some differences were observed when compared with the MONT-OTC spectrum (Fig. 2C). These differences included, in addition to sharper resonance of some signals, a new resonance vicinal to the one corresponding to C_9 (Fig. 2A and C). This new resonance suggested the existence of new species in MONT-Ca-OTC as previously proposed [38]. Due to low spectral resolution, further insight on the nature of those species would require further spectroscopic probing, for example via [43] Ca NMR.

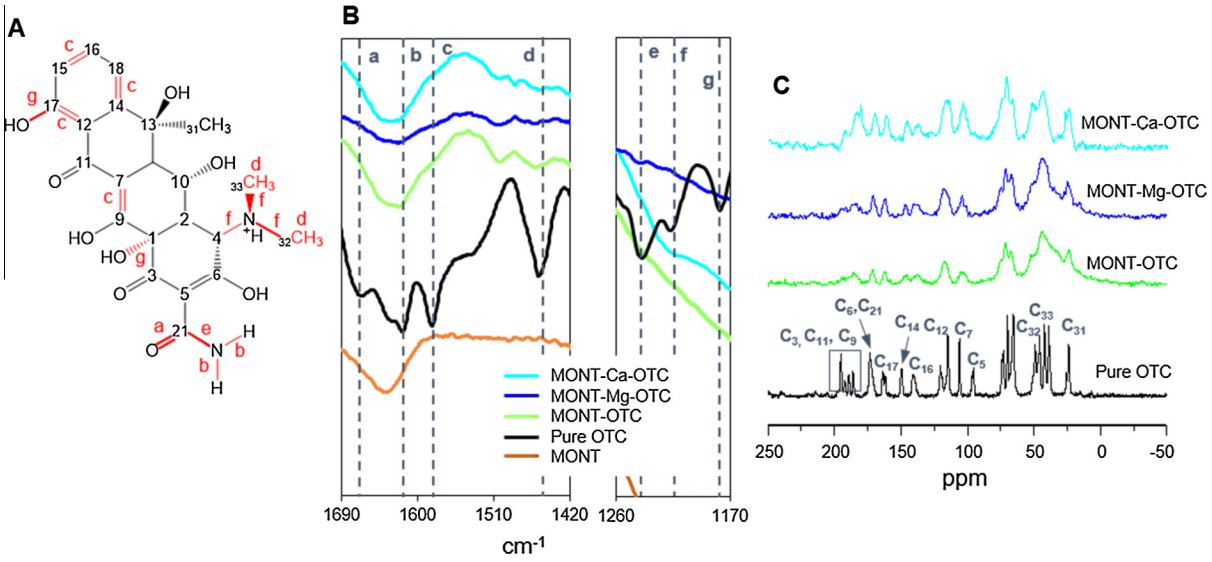

Fig. 2. Structure of OTC (A), and FTIR (B) and $^{1}H–^{13}C$ CPMAS NMR (C) spectra of Na-MONT with OTC in the absence and presence of Ca or Mg at pH 8. The OTC structure shows the assigned IR vibration bands (a–g) and the numbers assigned to the C atoms illustrated on the NMR spectrum. The dashed lines in B show the IR vibration bands corresponding to the letters on the OTC structure. Color legend for spectra in B and C: MONT alone (brown), OTC alone (black), OTC with Na-MONT (MONT-OTC, green), OTC-Mg with Na-MONT (OTC-Mg-MONT, dark blue), OTC-Ca with Na-MONT (OTC-Ca-MONT, light blue).

In sum, despite the more than twofold increase in adsorbed OTC in the presence of the divalent cations, our NMR results indicated immobilization of Mg-OTC and Ca-OTC at the MONT surface similar to adsorbed OTC in the absence of divalent metal cations and, in the case of Ca-OTC, some new species present in low amount relative the total amount of adsorbed species. Thus, our spectroscopic data obtained via both FTIR and NMR did not provide strong evidence that an inner-sphere ternary complexation was significant in anchoring adsorbed OTC wherein the divalent cations would serve as a bridge between the antibiotic species and the clay surface. We therefore shifted our focus on elucidating the role of interlayer adsorption in facilitating OTC adsorption in the presence of divalent cations, specifically Mg.

3.3. Experimental XRD analysis

In agreement with previous studies [30–32,34–36], the pH-dependent OTC adsorption was correlated positively with intercalation within the MONT layers as revealed by XRD (Fig. 3). The high OTC adsorption at pH 4 (226 mmol OTC kg^{-1} clay) led to

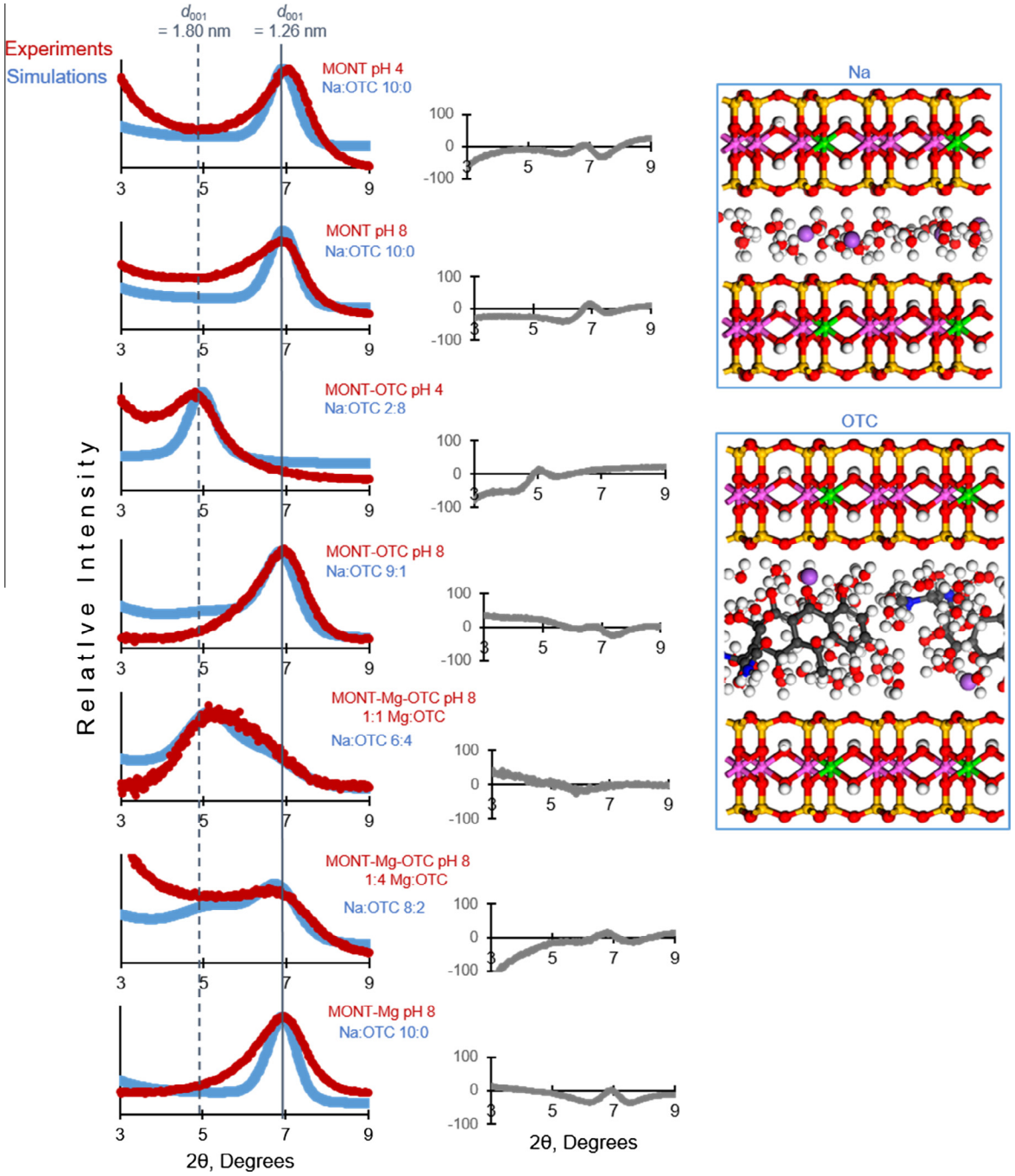

Fig. 3. Experimental (dark red) and simulated XRD (blue) spectra of MONT in the presence and absence of OTC and metal-OTC; the goodness of fit (simulated values–measured values) is shown in gray for each condition. The experimental spectra from top to bottom: MONT at pH 4, MONT at pH 8, MONT-OTC at pH 4, MONT-OTC at pH 8, MONT-Mg-OTC at pH 8 at 1:4 Mg:OTC reacting solution, MONT-Mg-OTC at pH 8 at 1:1 Mg:OTC reacting solution, and MONT-Mg at pH 8 (see Section 2 more details). Molecular-dynamics optimized MONT structures (shown on the right) were used to obtain simulated XRD assuming a partially segregated interstratification (see Section 2 for more details). The solid vertical line indicates d_{001} of 1.26 nm for Na-MONT interlayer without OTC and the dashed vertical line indicates d_{001} of 1.8 nm for MONT interlayers saturated with OTC. The MONT structures used in the simulated XRD were reprinted with permission from Ref. [34].

an expansion in the MONT d_{001} from ~1.26 to ~1.80 nm whereas the low OTC adsorption at pH 8 (54 mmol OTC kg^{-1} clay) only induced marginal change in the d_{001} (Fig. 3). In addition, we show here that, the aforementioned 120% increase in OTC adsorption in the presence of a 1:1 Mg:OTC solution at pH 8 was coupled with a shift in d_{001} from 1.28 nm to 1.72 nm, thus illustrating an increase in interlayer adsorption in the presence of Mg (Fig. 3).

To probe further the role of Mg in facilitating the interlayer adsorption, we obtained the XRD pattern of MONT following reaction with solutions containing 1:4 Mg:OTC solution or only Mg (Fig. 3). When the Mg:OTC ratio was lowered from 1:1 to 1:4, we found that the extent of the interlayer adsorption was greatly reduced. This was characterized by a decrease in the d_{001} from ~1.70 nm to ~1.28 nm. There was also a large broadening of the 001 peak in the XRD profiles of the MONT-Mg-OTC structures (Fig. 3), which was consistent with a segregated interstratification pattern as previously proposed for OTC intercalated within Ca-MONT [34,38]. In the absence of OTC, the XRD pattern of the MONT with adsorbed Mg resulted in an XRD pattern with a broad peak centered on the same d_{001} value obtained for Na-MONT in the absence of OTC; such broadening was indicative of the co-presence of Mg-populated interlayers with the predominant Na-populated interlayers (Fig. 3).

Our experimental XRD profiles thus revealed that the co-sorption of Mg with OTC was a pre-requisite to the enhanced interlayer adsorption of OTC. This interlayer adsorption, as indicated by our spectroscopic data, was achieved by a cation-exchange mechanism on the basal clay surface similar to OTC adsorption in the absence of the divalent metal cations [25,31,34]. This may explain the similar interstratification pattern previously reported for the XRD patterns of Na-MONT and Ca-MONT intercalated with OTC [38]. Therefore, we looked into modeling interstratification patterns in the presence of Mg by taking into account molecular dynamics-optimized adsorptive conformations of the OTC in Na-MONT interlayers [34].

3.4. Interlayer characterization via simulated XRD analysis

Using model adsorptive conformations, simulated XRD profiles were obtained as detailed previously assuming a segregated pattern of interstratified layers of Na-MONT, with or without OTC-exchanged layers (Fig. 3) [34]. The goodness-of-fit between the model-estimated and experimentally-determined XRD patterns demonstrated that the theoretical layer compositions generally provided for adequate modeling of the XRD of the OTC-MONT structures (Fig. 3). These theoretical layer compositions were subsequently employed to characterize the structures obtained under our different experimental conditions.

As expected, the experimental XRD profiles of Na-MONT in the absence of OTC at pH 4 and pH 8 matched well the simulated XRD profiles for the stacking composition with 100% Na-MONT (Fig. 3). In the presence of adsorbed OTC at pH 4, a simulated stacking with 80% OTC-exchanged MONT layers was required to obtain a similar d_{001} as the experimental XRD (Fig. 3). On the other hand, the minimal interlayer adsorption at pH 8 was characterized by a simulated stacking with 10% OTC-exchanged MONT layers, indicating that the majority of the OTC adsorbed was not within the interlayer [31,34] (Fig. 3). Therefore, our simulations revealed that the 76% decrease in the amount of OTC adsorbed from pH 4 to pH 8 was accompanied by an 87.5% reduction in OTC-containing MONT interlayers, thus confirming that OTC adsorption on MONT is facilitated by access of OTC to the MONT interlayers (Figs. 1B and 3B).

The increase in OTC adsorption in the presence of Mg was also characterized by the simulated segregated interstratified layers (Fig. 3B). As previously mentioned, we have measured a 120% increase in OTC adsorbed when OTC was introduced with a 1:1 Mg:OTC solution at pH 8 (Fig. 1B). According to the XRD simulations, this increase was coupled with a 200% increase (from 20% to 60%) in the amount of OTC-containing MONT layers (Fig. 3). Importantly, a 75% decrease in Mg concentration relative to OTC (from 1:1 to 1:4 Mg:OTC) led to a 67% decrease in OTC-exchanged MONT interlayers (Fig. 3). And, when OTC was absent and Mg was the same as in the 1:1 Mg:OTC, the measured XRD profile was reminiscent of the simulated XRD of a stacking composition containing 100% Na-MONT with no OTC (Fig. 3). In sum, the combined findings from our experimental and simulated XRD profiles led us to the conclusion that the co-presence of Mg and OTC altered the aggregation of the MONT layers to promote interlayer adsorption of OTC.

3.5. Concluding remarks

Similar adsorption isotherms were reported for the adsorption of three different types of TC antibiotics including OTC on Na-MONT [25]. Therefore, our insights on OTC adsorption in the presence of divalent cations would be also relevant to understanding the adsorption behavior of other TCs and related antibiotics. In the Introduction, we put forth three hypothesized roles of divalent metal cations in promoting OTC adsorption on Na-MONT under circumneutral and basic pH conditions: (1) bridges in a ternary complex; (2) promotion of interlayer interstratification; (3) modifications of the mineral aggregation chemistry. The formation of a ternary complex mediated by a divalent cation bridge was proposed as the primary mechanism responsible for increased adsorption of tetracycline antibiotics to clay surfaces [25,38]. Our spectroscopic data revealed that the dimethyl amino group was involved in mediating OTC adsorption both in the absence [31] and presence of divalent cations. These data, however, did not support the occurrence of a strong ternary complex as a requisite to the promoted OTC adsorption, albeit an outer-sphere bridging complexation may be possible. Instead, in support of the second mechanism, interlayer adsorption was found to be a required phenomenon in the divalent cation-promoted adsorption.

Using simulated XRD profiles, we were able to characterize the interstratified layers as a segregated combination of OTC-intercalated interlayers and Na- or Mg-populated interlayers. The present insights highlight the need to expand the mechanistic framework in subsequent studies on how the specific aqueous conditions can lead to enhanced interlayer trapping of ionizable organic molecules including antibiotics within smectite-type clay minerals in natural and engineered soil matrices. Our findings imply that the ubiquitous presence of multivalent cations in the soil matrix may facilitate interlayer trapping of TC antibiotics in clay-enriched soils by modifying the aggregation chemistry of the clay layers, thus highlighting the possible importance of the third mechanism. To practically implement this adsorption process in engineering antibiotic adsorbents, however, further structural insights are needed. In particular, the aqueous structures of the adsorbates as well as the alterations in the clay crystallites that evolve from the co-sorption of the divalent cations with the antibiotic species warrant further characterization.

Acknowledgements

We are grateful to Delphine Tisserand and Florian Molton of the University of Grenoble for technical assistance. This research was supported in parts by a start-up package from Cornell University and a Fulbright Scholarship, both awarded to L.A.

References

[1] R. Hirsch, T. Ternes, K. Haberer, K.L. Kratz, Occurrence of antibiotics in the aquatic environment, Sci. Total Environ. 225 (1999) 109.

[2] K. Kümmerer, Pharmaceuticals in the Environment; Sources, Fate, Effects and Risks, Springer, New York, 2001.
[3] D.W. Kolpin, E.T. Furlong, M.T. Meyer, E.M. Thurman, S.D. Zaugg, L.B. Barber, H. T. Buxton, Pharmaceuticals, hormones, and other organic wastewater contaminants in U.S. streams, 1999–2000: a national reconnaissance, Environ. Sci. Technol. 36 (2002) 1202.
[4] E.R. Long, M. Dutch, S. Weakland, B. Chandramouli, J.P. Benskin, Quantification of pharmaceuticals, personal care products, and perfluoroalkyl substances in the marine sediments of Puget Sound, Washington, USA, Environ. Toxicol. Chem. 32 (2013) 1701.
[5] G. Hamscher, S. Sczesny, H. Hoper, H. Nau, Determination of persistent tetracycline residues in soil fertilized with liquid manure by high-performance liquid chromatography with electrospray ionization tandem mass spectrometry, Anal. Chem. 74 (2002) 1509.
[6] X.-S. Miao, F. Bishay, M. Chen, C.D. Metcalfe, Occurrence of antimicrobials in the final effluents of wastewater treatment plants in Canada, Environ. Sci. Technol. 38 (2004) 3533.
[7] S. Kim, P. Eighhorn, J.N. Jensen, A.S. Weber, D.S. Aga, Removal of antibiotics in wastewater: effect of hydraulic and soil retention times on the fate of tetracycline in the activated sludge process, Environ. Sci. Technol. 39 (2005) 5816.
[8] C. McKinney, K. Loftin, M.T. Meyer, J.G. Davis, A. Pruden, *Tet* and *sul* antibiotic resistance genes in livestock lagoons of various operation type, configuration, and antibiotic occurrence, Environ. Sci. Technol. 44 (2010) 6102.
[9] S.R. Joy, S.L. Bartelt-Hunt, D.D. Snow, J.E. Gilley, B.L. Woodbury, D.B. Parker, D.B. Marx, X. Li, Fate and transport of antimicrobials and antimicrobial resistance genes in soil and runoff following land application of swine manure slurry, Environ. Sci. Technol. 47 (2013) 12081.
[10] H. Fang, H. Wang, L. Cai, Y. Yu, Prevalence of antibiotic resistance genes and bacterial pathogens in long-term manured greenhouse soils as revealed by metagenomic survey, Environ. Sci. Technol. 49 (2015) 1095–1104.
[11] F.-J. Peng, L.-J. Zhou, G.-G. Ying, Y.-S. Liu, J.-L. Zhao, Antibacterial activity of the soil-bound antimicrobials oxytetracycline and ofloxacin, Environ. Toxicol. Chem. 33 (2014) 776.
[12] S.A. Sassman, L.S. Lee, Sorption of three tetracyclines by several soils: assessing the role of pH and cation exchange, Environ. Sci. Technol. 39 (2005) 7452.
[13] J.C. Carlson, S.A. Mabury, Dissipation kinetics and mobility of chlortetracycline, tylosin, and monensin in an agricultural soil in Northumberland CountMy, Ontario, Canada, Environ. Toxicol. Chem. 25 (2006) 1–10.
[14] S.-C. Kim, K. Carlson, Temporal and spatial trends in the occurrence of human and veterinary antibiotics in aqueous and river sediment matrices, Environ. Sci. Technol. 41 (2007) 50.
[15] Y. Zielezny, J. Groeneweg, H. Vereecken, W. Tappe, Impact of sulfadiazine and chlorotetracycline on soil bacterial community structure and respiratory activity, Soil Biol. Biochem. 38 (2006) 2372.
[16] B. Halling-Sørensen, Inhibition of aerobic growth and nitrification of bacteria in sewage sludge by antibacterial agents, Arch. Environ. Contam. Toxicol. 40 (2001) 451.
[17] S. Boleas, C. Alonso, J. Pro, C. Fernández, G. Carbonell, J.V. Tarazona, Toxicity of the antimicrobial oxytetracycline to soil organisms in a multi-species-soil system (MS center dot 3) and influence of manure co-addition, J. Hazard. Mater. 122 (2005) 233.
[18] S. Thiele-Bruhn, I.-C. Beck, Effects of sulfonamide and tetracycline antibiotics on soil microbial activity and microbial biomass, Chemosphere 59 (2005) 457.
[19] C.J. Wilson, R.A. Brain, H. Sanderson, D.J. Johnson, K.T. Bestari, P.K. Sibley, K.R. Solomon, Structural and functional responses of plankton to a mixture of four tetracyclines in aquatic microcosms, Environ. Sci. Technol. 38 (2004) 6430.
[20] H.E. Goetsch, S.E. Mylon, S. Butler, J.L. Zilles, T.H. Nguyen, Oxytetracycline interactions at the soil-water interface. Effects of environmental surfaces on natural transformation and growth inhibition of *Azotobater vinelandii*, Environ. Toxicol. Chem. 32 (2012) 2217.
[21] A. Thiele-Bruhn, Microbial inhibition by pharmaceutical antibiotics in different soils—dose-response relations determined by the iron (III) reduction test, Environ. Toxicol. Chem. 24 (2005) 869.
[22] D.H. Kang, S. Gupta, C. Rosen, V. Fritz, A. Singh, Y. Chander, H. Murray, C. Rohwer, Antibiotic uptake by vegetable crops from manure-applied soils, J. Agric. Food Chem. 61 (2013) 9992.
[23] M. Pan, C.K.C. Wong, L.M. Chu, Distribution of antibiotics in wastewater-irrigated soils and their accumulation in vegetable crops in the Pearl River Delta, Southern China, J. Agric. Food. Chem. 62 (2014) 11062.
[24] A.D. Jones, G.L. Bruland, S.G. Agrawal, D. Vasudevan, Factors influencing the sorption of oxytetracycline to soils, Environ. Toxicol. Chem. 24 (2005) 761.
[25] R.A. Figueroa, A. Leonard, A.A. Mackay, Modeling tetracycline antibiotic sorption to clays, Environ. Sci. Technol. 38 (2004) 476.
[26] A.J. Carasquillo, G.L. Bruland, A.A. MacKay, D. Vasudevan, Sorption of ciprofloxacin and oxytetracycline zwitterions to soils and soil minerals: influence of compound structure, Environ. Sci. Technol. 42 (2008) 7634.
[27] J. Wang, J. Hu, S. Zhang, Studies on the sorption of tetracycline onto clays and marine sediment from seawater, J. Colloid. Interf. Sci. 349 (2010) 578.
[28] G. Sposito, The Chemistry of Soils, second ed., Oxford University Press, New York, 2008.
[29] I.C. Bourg, G. Sposito, Ion exchange phenomena, in: P.M. Huang, Y. Li, M.E. Summer (Eds.), Handbook of Soil Science, Properties and Processes, second ed., CRC Press, Boca Raton, 2011 (Chapter 16).
[30] P. Kulshrestha, R.F. Giese Jr., D.S. Aga, Investigating the molecular interactions of oxyteracycline in clay and organic matter: insights on factors affecting its mobility in soil, Environ. Sci. Technol. 38 (2004) 4097.
[31] L. Aristilde, C. Marichal, J. Miéhé-Brendlé, B. Lanson, L. Charlet, Interactions of oxytetracycline with a smectite clay: a spectroscopic study with molecular simulations, Environ. Sci. Technol. 44 (2010) 7839.
[32] Z. Li, V.M. Kolb, W.-T. Jiang, H. Hong, FTIR and XRD investigations of tetracycline intercalation in smectites, Clays Clay Miner. 4 (2010) 462.
[33] M.E. Parolo, M.C. Savini, J.M. Vallés, M.T. Baschini, M.J. Avena, Tetracycline adsorption on montmorillonite: pH and ionic strength effects, Appl. Clay Sci. 40 (2008) 179.
[34] L. Aristilde, B. Lanson, L. Charlet, Interstratified layers from the pH-dependent intercalation of a tetracycline antibiotic within smectite clay layers, Langmuir 29 (2013) 4492.
[35] P.-H. Chang, J.-S. Jean, W.-T. Jiang, Z. Li, Mechanisms of tetracycline on rectorite, Colloid Surf. A 339 (2009) 94.
[36] J. Pils, D.A. Laird, Sorption of tetracycline and chlortetracycline on K- and Ca-saturated soil clays, humic substances and clay humic complexes, Environ. Sci. Technol. 41 (2007) 1928.
[37] Y.J. Wang, D.-A. Jia, R.-J. Sun, H.-W. Zhu, D.-M. Zhou, Adsorption and cosorption of tetracycline and copper(II) on montmorillonite as affected by solution pH, Environ. Sci. Technol. 42 (2008) 3254.
[38] M.E. Parolo, M.J. Avena, G.R. Pettinari, M.T. Baschini, Influence of Ca^{2+} on tetracycline adsorption on montmorillonite, J. Colloid Interf. Sci. 368 (2012) 420.
[39] L. Aristilde, G. Sposito, Molecular modeling of metal complexation by a fluoroquinolone antibiotic, Environ. Toxicol. Chem. 27 (2008) 2304.
[40] R. Glaeser, J. Méring, Isothermes d'hydration des montmorillonites bi-ioniques (Na, Ca), Clay Miner. Bull. 2 (1954) 188.
[41] J.L. McAtee, Heterogeneity of montmorillonite, Clays Clay Miner. 5 (1956) 279.
[42] D.H. Fink, F.S. Nakayama, B.L. McNeal, Demixing of exchangeable cations in free-swelling bentonite clay, Soil Sci. Soc. Am. Proc. 35 (1971) 552.
[43] I. Shainberg, N.I. Alperovitch, R. Keren, Charge density and Na–K–Ca exchange on smectites, Clays Clay Miner. 35 (1987) 68.
[44] T. Iwasaki, T. Watanabe, Distribution of Ca and Na ions in dioctahedral smectites and interstratified dioctahedral mica/smectites, Clays Clay Miner. 36 (1988) 73.
[45] B. Lanson. Modelling of X-ray diffraction profiles: Investigation of defective lamellar structures crystal chemistry, in: M.F. Brigatti, A. Mottana (Eds.), European Mineralogical Union Notes in Mineralogy, Layered Mineral Structures and their Applications in Advanced Technologies, vol. 11, European Mineralogical Union & Mineralogical Society UK & Ireland, London, 2011 (Chapter 4).
[46] A. Géhin, J.M. Grenèche, C. Tournassat, J. Brendlé, D.G. Rancourt, L. Charlet, Reversible surface-sorption-induced electron transfer oxidation of Fe(II) at reactive sites on a synthetic clay mineral, Geochim. Cosmochim. Acta 71 (2007) 863.
[47] S. Tongaree, D.R. Flanagan, R.I. Poust, The interactions between oxytetracycline and divalent metal ions in aqueous and mixed solvent systems, Pharm. Dev. Technol. 4 (1999) 581.